ACADÉMIE
DES SCIENCES
INSTITUT DE FRANCE

Comptes Rendus

Géoscience

Sciences de la Planète

Pascal Marquet

The absolute seawater entropy: Part II. Case studies

Volume 358 (2026), p. 255-269

https://doi.org/10.5802/crgeos.334

The Comptes Rendus. Géoscience — Sciences de la Planète *are a member of the Mersenne Center for open scientific publishing*
www.centre-mersenne.org — e-ISSN : 1778-7025

ACADÉMIE DES SCIENCES
INSTITUT DE FRANCE

Comptes Rendus. Géoscience — Sciences de la Planète
2026, Vol. 358, p. 255-269
https://doi.org/10.5802/crgeos.334

Research article
Oceanography, oceanic biogeosciences

The absolute seawater entropy: Part II. Case studies

Pascal Marquet [a]

[a] Retired in Toulouse, France
URL: https://sites.google.com/view/pascal-marquet
E-mail: pascalmarquet@yahoo.com

Abstract. The aim of this second part of the article is to study the absolute definition of the seawater entropy described in Part I with several concrete cases. Observed vertical profiles and polar transects, as well as analysed surface data, show that very different temperatures and salinity values can organise to create new isentropic regions. This can only be revealed by the absolute formulation of the entropy of seawater (Arctic Ocean; Bay of Bengal; Mediterranean, Black, and Caspian Seas). Existing hypotheses to explain these results include the possible impact of turbulent processes that must be applied to the entropies of the atmosphere and oceans.

Keywords. Entropy, Third law, Thermodynamics, Potential temperature, Isentropic surface.
Manuscript received 7 October 2024, revised 30 November 2025 and 24 March 2026, accepted 25 March 2026.

1. Introduction

The present Part-II paper follows on from the Part-I paper (Marquet, 2026), in which the absolute entropy of the ocean η_{abs} (expressed in $J{\cdot}K^{-1}{\cdot}kg^{-1}$) was defined as a modification of the standard arbitrary TEOS10 version $\eta_{std/TEOS10}$ (see McDougall, Feistel, et al., 2010), according to

$$\eta_{abs} = \eta_{std/TEOS10} + \Delta\eta_s, \tag{1}$$

$$\Delta\eta_s = (\eta_{s0} - \eta_{w0}) \times \frac{(S_A - S_{SO})}{1000}, \tag{2}$$

$$\eta_{w0} \approx 3513.4 \pm 1.7\ J{\cdot}K^{-1}{\cdot}kg^{-1} \quad (\text{at } 0\ ^\circ C), \tag{3}$$

$$\eta_{s0} \approx 1633.3 \pm 15\ J{\cdot}K^{-1}{\cdot}kg^{-1} \quad (\text{at } 0\ ^\circ C), \tag{4}$$

$$\Delta\eta_s \approx (-1880 \pm 17) \times \frac{(S_A - S_{SO})}{1000}, \tag{5}$$

where η_{w0} and η_{s0} are the absolute entropies for pure water and sea salts (respectively), S_A is the absolute salinity (in $g{\cdot}kg^{-1}$), and $S_{SO} = 35.16504\ g{\cdot}kg^{-1}$ is the standard value for which the standard TEOS10 seawater entropy is cancelled at the ambiant temperature $t_{S0} = 0\ ^\circ C$ by using arbitrary tuning values for both η_{w0} and η_{s0}.

The aim of this second part is to demonstrate the physical meaning of this new absolute definition η_{abs} by studying the impacts of the salinity increment $\Delta\eta_s$ on observed oceanic vertical profiles and analysed datasets. It is shown that the absolute version of the seawater entropy allows the observed data to be described in a new light. In particular, new isentropic regions both vertically and horizontally can only be revealed by the absolute and thermodynamically consistent definition of the seawater entropy.

The paper is organised as follows. In the next Section 2 are shown several numerical applications of the absolute seawater entropy, with: in Subsection 2.1 a study of a CTD (cast 43) vertical profile observed during SCICEX'96, with surface, Pacific, and Atlantic layers; in Subsection 2.2 a study of two SCICEX'97 vertical transects; and in Subsections 2.3 to 2.6 studies of the WOA23 analysed surface conditions at global and regional scales (Arctic Ocean, Bay of Bengal, Mediterranean, Black, and Caspian Seas). It appears that the classic $t - S_A$ ocean diagrams can be improved, with both the old isopycnic (iso-potential-density) lines and the new absolute iso-entropy lines,

to show remarkable alignments of points along these two families of curves.

Finally, in Section 3 I review the main results of the study and point out that turbulent processes may provide part of the explanation for these homogenisations of absolute seawater entropy, following the old Richardson's recommendations (Richardson, 1919; Richardson, 1922) that atmospheric and oceanic turbulence should apply to absolute entropy and not to temperature.

2. Numerical applications

2.1. *The SCICEX'96 experiment*

To maximise the chances of observing significant impacts of salinity on absolute entropy profiles, it was necessary to find a well-documented example of an oceanic profile with both large variations in salinity and small variations in temperature. The vertical profiles shown in the Figures 1, already plotted by Steele et al. (2004, his Fig. 1, p. 2), can serve this purpose.

The aim of the paper by Steele et al. (ibid.) was to study the circulation and interannual variability of summertime Pacific origin halocline waters in the Arctic Ocean, with the SCICEX'96 [1] (cast 43) CTD vertical profiles typical of the Canadian Basin shown in Figure 1. This vertical profile is made of the "summer Pacific halocline water" layer (2), with a subsurface temperature maximum located in between the mixed "surface layer" (1) and the deeper "Atlantic layer" (3).

In the top panels are plotted[2]: (i) the "Celsius temperature" t (bold solid red, and T (abs) in thin dashed purple); (ii) the "potential temperature" θ (bold solid blue); (iii) the seawater "conservative temperature" Θ (thin solid red); and (iv) the salinity (thin solid blue). Top Figures 1 show that the high-resolution profiles indeed correspond (on average and below the large-temperature first 20 m depth layer) to the mean profiles plotted in Fig. 1 of Steele et al. (ibid.).

The Celsius, potential, and conservative temperatures overlap almost exactly (up to less than 0.04 °C), with therefore very few differences in this Arctic case. This result is likely due to the small variations in temperature in this case, where t remains between -1.6 °C and -0.4 °C.

Similarly, the bottom left part of Figure 1 shows that the structure of the vertical profile of the standard seawater entropy (in blue)[3], apart from changes in units, remains very close to that of the vertical temperature profile, with very little impact from strong variations in salinity. In particular, the values of the Pacific halocline layer (2) are larger than both the surface layer (1) and deep Atlantic layer (3), with values in (3) increasing with the depth for both the TEOS10 entropy and the Celsius temperature.

The fact that the TEOS10's version of the seawater entropy profiles closely resembles those of temperature can be understood as follows. Firstly, the impact of salinity S_A must be very low in the TEOS10's version, due to the hypothesis $(\eta_{s0} - \eta_{w0}) = 0$ and thus $\Delta\eta_s = 0$. Secondly, entropy must vary like the logarithm of absolute temperature via $C_p \ln(T/\overline{T})$, to within a constant. We can translate small variations in $T' = T - \overline{T} = t'$ by the second-order approximation $\ln(1+x) \approx x - x^2/2 + \cdots$, and thus the first-order result $\eta \approx (C_p/\overline{T})\ t' + \text{cste}$. This shows that the absolute seawater entropy is approximately proportional to $t' \approx 1$ °C up to the quadratic term $-x^2/2$, and thus up to about $t'/(2\,\overline{T}) \approx 0.5/273 \approx 0.2\%$.

Differently, the vertical profile of absolute seawater entropy (in red) shows different behaviors, with a decrease with the depth of the absolute entropy of the layer (1), then (2) and (3). Note that the uncertainty of the impact of $\Delta\eta_s$ is small (not shown), because the relative uncertainty of -1880 ± 17 in (5) represents only 1% of the difference between the blue and red curves in Figure 1.

In addition, the deep layer (3) becomes nearly isentropic with the absolute entropy formulation, due to compensation for temperature and salinity gradients that do not occur with the current TEOS10

[1] The general webpage of the "SCICEX" (Science Ice Exercise) is https://nsidc.org/scicex/scicex-data, with all the vertical CTD profiles available on the page https://www.nodc.noaa.gov/archive/arc0021/0000568/1.1/data/0-data/ (Submarine Arctic Science Program).

[2] The variables θ and Θ are computed via the subroutines `gsw_pt0_from_t(S_A,t,p)` and `gsw_ct_from_t(S_A,t,p)` in the TEOS10-GSW software, from which the "potential enthalpy" h^0 may be computed as $3991.868 \times \Theta$ J·kg^{-1} (McDougall, 2003; McDougall, Barker, et al., 2023).

[3] The standard TEOS10-GSW seawater entropy is computed via the subroutine `gsw_entropy_from_t(S_A,t,p)` in the TEOS10-GSW software.

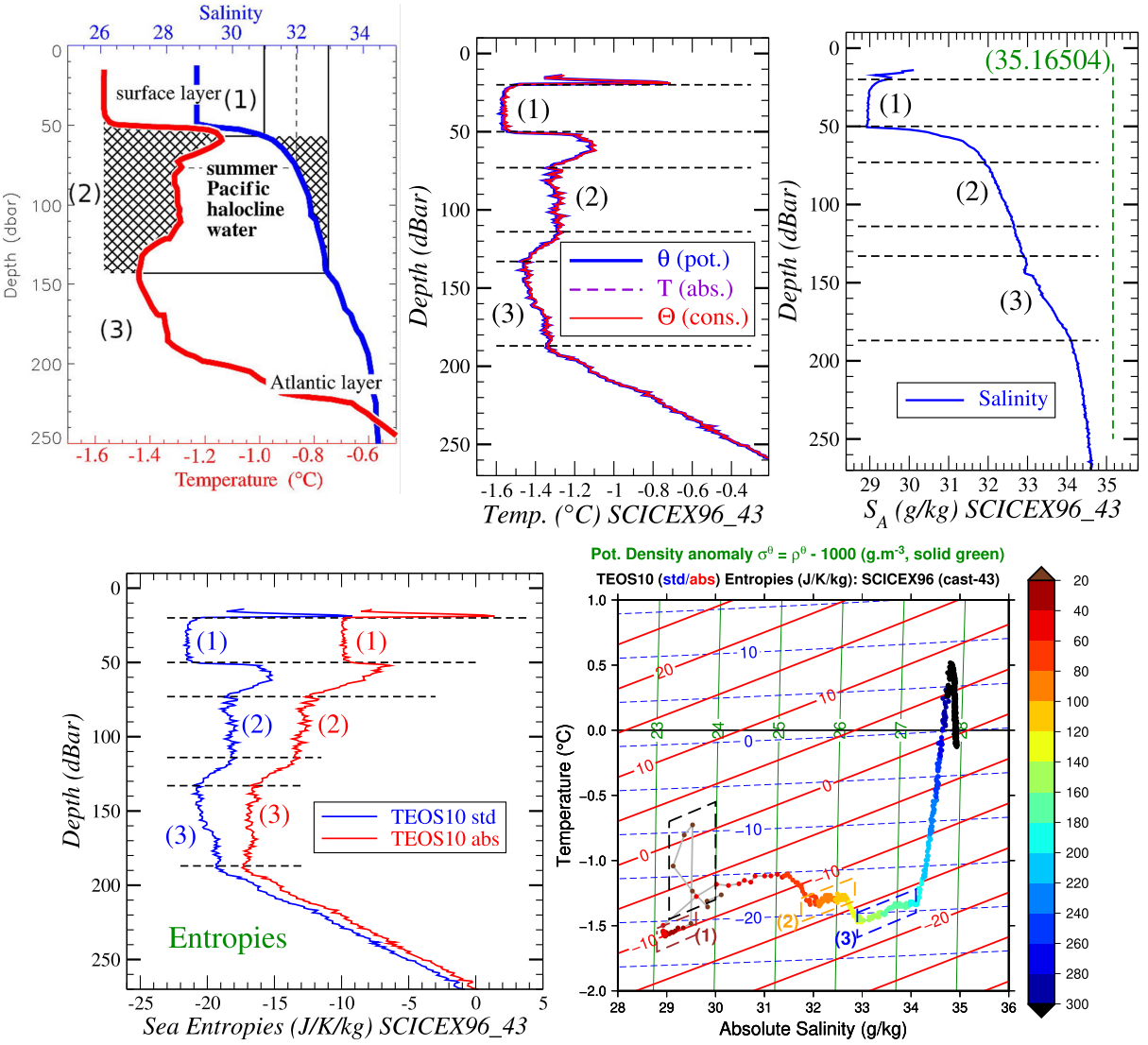

Figure 1. Top (left): an annotated version of Fig. 1 of Steele et al. (2004, AGU grants) corresponding to a study of the low-resolution SCICEX'96 (cast 43) CTD vertical profiles. Top (middle and right): the corresponding full-resolution vertical profiles for the potential temperature (θ, solid blue), Celsius temperature (T, dashed purple), conservative temperature (Θ, solid red), and salinity (solid blue), with $S_{SO} = 35.16504$ g·kg^{-1} the TEOS10 standard salinity (green), for the high-resolution SCICEX'96 CTD (cast 43) vertical profiles. Bottom (left): the corresponding standard (solid blue) and absolute (solid red) versions of the seawater entropy, with the absolute mean value of the salinity increment $\Delta\eta_S$ given by (5). Bottom (right): the same $t-S_A$ diagram as in the Figs. 1 of Part I, with the (almost horizontal) TEOS10's standard entropy (thin blue dashed lines), with the (more slantwise) TEOS10's absolute entropy (thick red solid lines), and with the plot of the SCICEX'96 (cast 43) vertical profile coloured from dark brown to dark blue for the depth from 14 m to 300 m, and then in black up to the last 1004 m depth.

(arbitrary reference values) formulation. The same is true at the top of the surface layer (1), where the increase in both temperature and salinity creates an extended absolute isentropic region including the 23 and 19 m layers, where the values of the standard TEOS10 entropy start to increase.

Another way to illustrate these features is the $t-S_A$ diagram plotted in the bottom right part of Figure 1, which shows in an interesting new way the three absolute isentropic regions (1), (2), and (3) that are clearly aligned along the new set of absolute isentropic red lines (see the three brown, orange, and

blue dashed boxes), which cannot be due to chance. The points are linked by a grey line in order to show how the upper levels are organised with a double loop (within the black dashed box) above and below the layer (1). The green isopycnic (potential-density anomaly) lines are almost vertical and are not useful for studying the upper layers (1), (2), and (3), even though the deep-layer points (z < 190 m depth) roughly converge toward the isopycnic line $\sigma^\theta \approx 27.8$ g·m^{-3}.

There may therefore be a double set of physical constraints illustrated by the two sets of curves in the $t - S_A$ diagrams: following either the absolute-isentropic red lines or the isopycnic lines (iso-pot.-density, in green), as confirmed by the other similar results shown in the next subsections.

The standard TEOS10 entropy (dashed thin blue) lines are almost isothermal lines for temperatures between −2 °C and +1 °C. The black points and dashed box represent the very surface atypical conditions (between 14 and 19 m depth). The graphical study of vertical ocean profiles could therefore be revisited thanks to this kind of classical $t-S_A$ diagram, but only if including the new set of red lines to reveal the absolute isentropic regions.

The absolute isentropic conditions of these three layers (1), (2) and (3) can also be understood from (2), (5), and with the first-order result $\eta \approx (C_p/\overline{T})\ t' + \text{cste}$. It is indeed possible to provide a first-order condition ($\delta\eta = 0$) for the respective impacts of joint variations in temperature (δt) and salinity (δS_A), leading to

$$\frac{C_p}{\overline{T}} \times \delta t \leftrightarrow -\frac{(\eta_{s0} - \eta_{w0})}{1000} \times \delta S_A^A,$$

$$14 \times \delta t = 1.88(7.4 \times \delta t) \leftrightarrow 1.88(\delta S_A), \quad (6)$$

$$\delta\eta \approx 1.88(7.4 \times \delta t - \delta S_A), \quad (7)$$

where $C_p \approx 4218$ J·K^{-1}·kg^{-1}, $\overline{T} \approx 300$ K, t' in °C and S_A in g·kg^{-1}. An application to the deep layer (3) for the SCICEX'96 (cast 43) CTD vertical profile corresponds to $\delta t \approx 0.17$ K and $\delta S_A \approx 1.2$ g·kg^{-1}, which from (6) indeed corresponds to $7.4 \times 0.17 = 1.26 \approx 1.2$ and to nearly isentropic conditions. Note that the draft value 14 in (6) agrees with the linear term in y in Table 1 in Part I: $[24715.571866078/(40 \times 40)] \times t \approx 15.4 \times t$. Note also that these relationships (6) and (7) are only valid for temperatures close to 0 °C, with $|y| = |t|/40 < 0.05$ small and thus with all the high-order terms depending on $y^2, y^3, \ldots$ duly neglected.

The presence of the surface fresh water with low salinity (here <30 g·kg^{-1}) results in a large increase in absolute entropy (+11.5 J·K^{-1}·kg^{-1}) for this SCICEX'96 cast 43 profile due to $\Delta\eta_s$, but with no impact on the usual TEOS10's version of entropy. However, these impacts cannot be arbitrary because, otherwise, there would be no point in measuring the entropy of the ocean. Indeed, the reference value $(\eta_{s0} - \eta_{w0})$ has clear impacts on (i) the difference in entropy between two points due to $(\Delta\eta_s)_2 - (\Delta\eta_w)_1$ and thus $(\eta_{s0} - \eta_{w0})/1000 \times [(S_A)_1 - (S_A)_2)]$; (ii) the gradient in entropy due to $(\eta_{s0} - \eta_{w0})/1000 \times \nabla S_A$; and (iii) the temporal evolution in entropy due to $(\eta_{s0} - \eta_{w0})/1000 \times [dS_A/dt]$. It is therefore not possible to consider that $(\eta_{s0} - \eta_{w0})$ could have no impact on the computation of a thermodynamic state function such as entropy; otherwise, this would be equivalent to denying this state function any physical meaning.

For instance, the second law of thermodynamics may imply, for suitable conditions, that the entropy should increase monotonically until it reaches its maximum at the state of thermodynamic equilibrium. But the search for such a "maximum entropy state" would be meaningless if one could modify at will the values of the seawater entropy, with, for instance, $\Delta\eta_s = 0$ presently assumed in the TEOS10 version and in all other present studies, with detrimental impacts in the entropy profiles in Figures 1. Similarly, the isentropic aspect of the deep layer (3) only appears with the absolute version of entropy, which is the only way of revealing this aspect, which acquires an obvious physical meaning and which cannot be modified by arbitrary choices of η_{s0} and η_{w0}, as presently made in TEOS10 and contrary to the third law of thermodynamics.

2.2. *The SCICEX'97 transects*

The properties highlighted on the sole vertical profiles of SCICEX'96 showing the interest of defining the seawater entropy in an absolute way (as suggested by thermodynamics) need to be confirmed on other examples. To do this, before studying even more global properties in the other sections, it is possible to study the SCICEX'97 transects, which are a kind of spatial extension of the SCICEX'96 profile.

I have retained 40 of the CTD0xx profiles to make the transect A shown in Figures 2, with xx from 05 to 52 (except the unusual noisy 15, 28, 33, 34, 48,

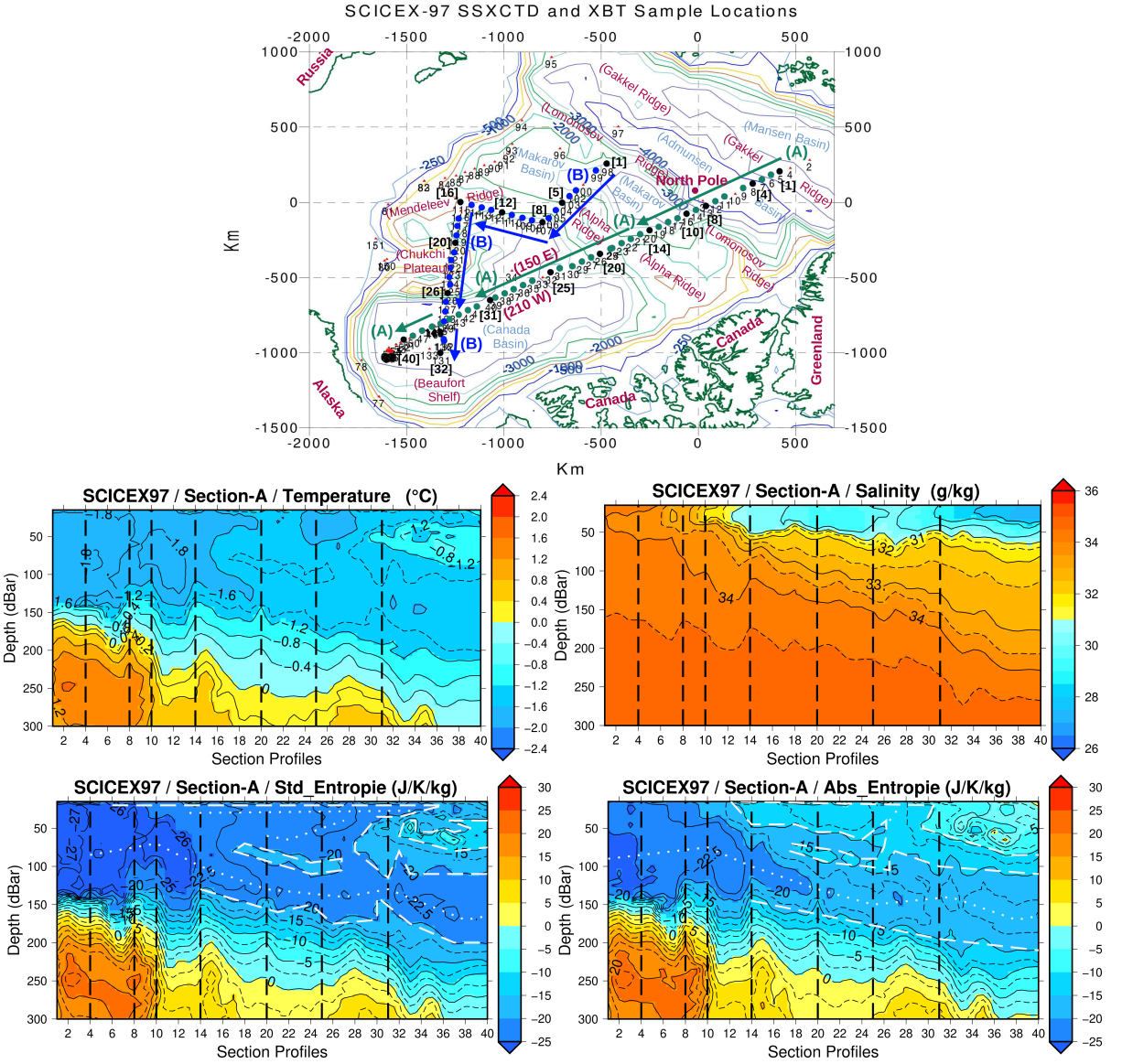

Figure 2. On the top: the annotated SCICEX-97 Sample Locations map (green points for the Transect-A and blue points for the Transect-B). Then the four Transect-A figures (from 15 m to 300 m depth) for the temperature (°C), salinity ($g \cdot kg^{-1}$), standard (TEOS10), and absolute (TEOS10+third-law) seawater entropies ($J \cdot K^{-1} \cdot kg^{-1}$).

49, and 51 CTD)[4]. I have retained 32 of the CTD0xxx profiles to make the transect B shown in Figures 3, with xxx from 098 to 129, 132, 136, and 131 (except the unusual noisy 100, 101, 116, 130, and 133 to 135 CTD)[5].

[4]The transect A (green points in the SCICEX-97 Sample Locations map) was roughly located along the longitude 150 E (210 W) and extended from the Gakkel Ridge (points [1]–[3] for CTD005 to CTD007); the Admunsen Basin (points [4]–[7]); the Lomonosov Ridge (close to the North Pole, points [8]–[10]); the Makarov Basin (points [11]–[13]); the Alpha Ridge (points [14]–[20]); the following Shelf (points [21]–[25]); and finally the Canada Basin (points [25]–[40]), passing close to the Chukchi Plateau (point [31]).

[5]The transect B (blue points in the SCICEX-97 Sample Locations map) extended from the Makarov Basin (points [1]–[4] for CTD098 to CTD102); the Alpha Ridge (points [5]–[7]); the

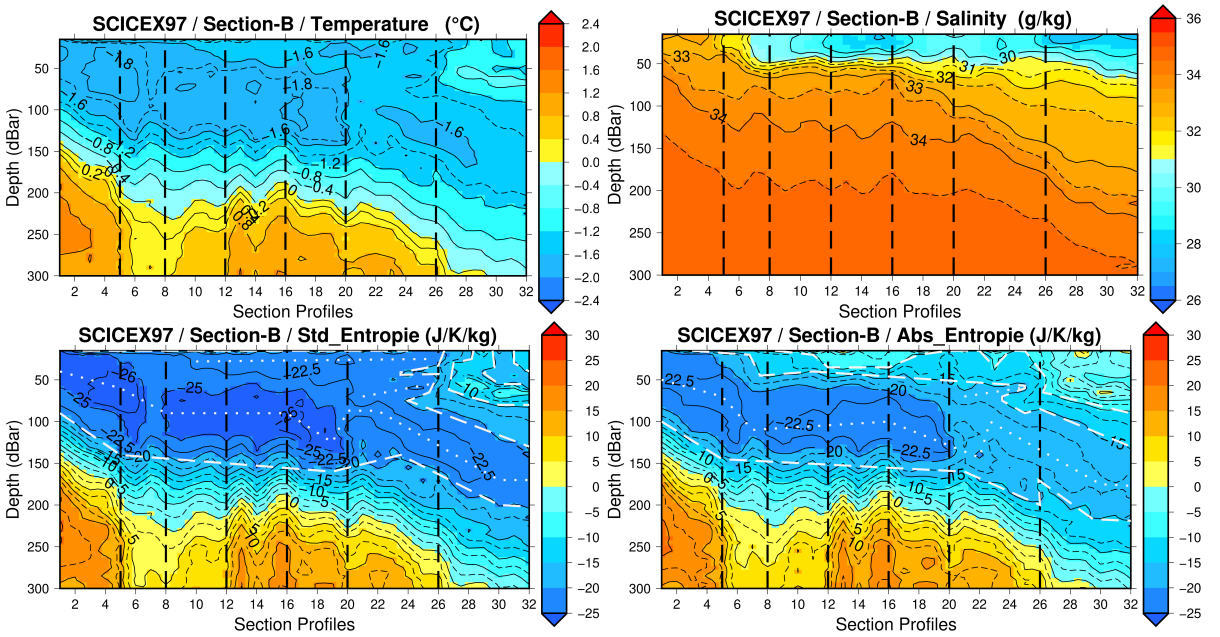

Figure 3. Same as for Figures 2, but for the Transect-B figures.

The two transects, A and B, exhibit almost the same properties, with a roughly north–south variation of the points and with an absolute (thermodynamic) version of the seawater entropy more interesting and more coherent spatially than the standard (TEOS10) arbitrary version.

Indeed, if the subsurface layer (between 15 and 150–200 m) is partly associated with the minimum of temperature (from −1.2 to −1.85 °C), it should also be modulated by the vertical gradient of salinity (from 28 to 34 g·kg^{-1}). But this is only the case due to the impact of the salinity increment $\Delta\eta_s$ on the absolute seawater entropy, which is to create a more coherent and unique subsurface layer with minimum values from −15 to −25 J·K^{-1}·kg^{-1}. Differently, the standard version shows a more uneven shape with a second layer (at about 30 m depth for all latitudes) largely influenced by the associated cold temperature tongue, without the thermodynamic impact of $\Delta\eta_s$ that creates the unique layer. There is also a clear deepening with decreasing latitudes for the absolute version (see the white dashed and dotted annotating lines).

Another interesting feature is the more coherent fresh surface layers with low salinity, with associated larger absolute values of the seawater entropy (light-blue and yellow colours, from −5 to +5 J·K^{-1}·kg^{-1}) and the greater values at the surface, whereas they are in a subsurface position for the standard (TEOS10) seawater entropy values (at about 60 m depth). We can see here the same impact already observed with the SCICEX'96 profile and layer (1), which has a higher absolute entropy than the other subsurface layers (2) and (3), whereas the opposite is true for the first layer (1), which has the lowest standard TEOS10 entropy.

All these differences confirm that the arbitrary definitions leading to the standard value of the TEOS10 entropy lead to significant differences in the spatial variations (in latitudes and depths) of the seawater entropy in comparison with its thermodynamic absolute definition. This could provide an incentive to plot and enrich future studies of this new thermodynamic variable, including the salinity increment term $\Delta\eta_s$.

2.3. *A study of global surface ocean entropy*

We cannot deduce from the study of the previous few examples that absolute entropy is of interest

Canada Basin Shelf (points [8]–[11]); the Mendeleev Ridge (points [12]–[16]); the Canada Basin Shelf (points [17]–[19]); the Chukchi Plateau (points [20]–[25]); and finally the Canada Basin (points [26]–[32]).

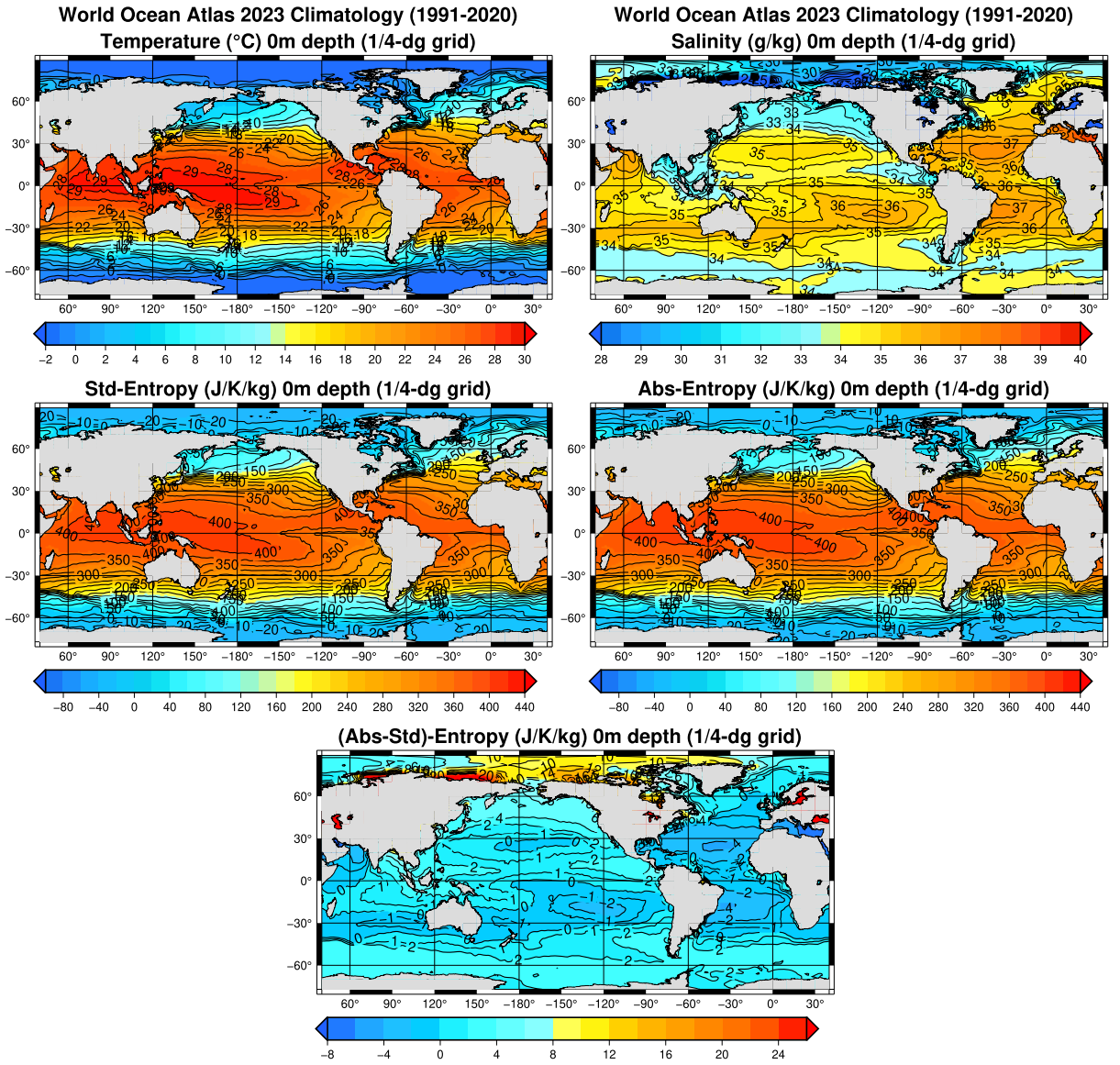

Figure 4. The 1991–2020 objectively analyzed annual surface means for the temperature, salinity, standard (Std) seawater entropy, absolute (Abs) seawater entropy, and difference (Abs–Std) in seawater entropy, computed from the World Ocean Atlas 2023 climatology (WOA23, release February 2024, quarter-degree grid). Documentation and data are available at https://www.ncei.noaa.gov/products/world-ocean-atlas.

elsewhere than in the polar regions, or even that it is of interest everywhere in these polar regions. We need to carry out other, more systematic, and therefore more global, studies.

At first sight, the global study shown in Figures 4 suggests that the surface mean standard (TEOS10) seawater entropy is almost everywhere similar to the absolute (third-law) version computed with the 1991–2020 annual means from the World Ocean Atlas 2023 (WOA23, quarter-degree resolution). This result is a priori somewhat disappointing, in the same ways as the potential and conservative temperatures almost overlap the absolute temperature for the SCICEX'96 vertical profile shown in Figure 1.

However, several differences can be guessed at the regional scale, such as those shown in Figures 5, 6,

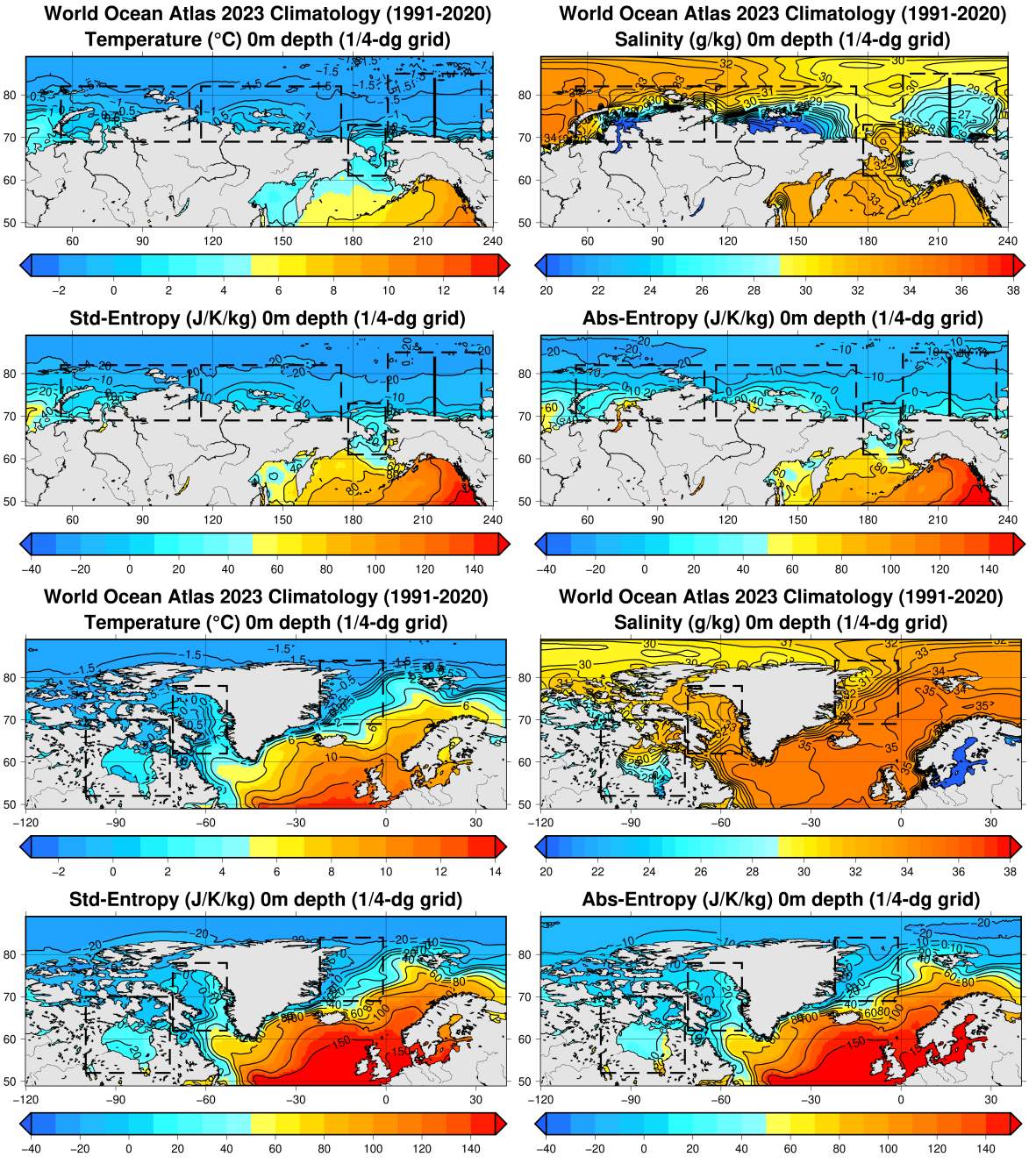

Figure 5. The same as in Figures 4, but for the Arctic Ocean.

and 7 and mainly corresponding to the regions with either large gradients in salinity or small (<32 g·kg^{-1}) or large (>37 g·kg^{-1}) values of the salinity itself, as shown in many places in the last panel of Figure 4 for the difference (Abs–Std) in seawater entropy (dark blue negative and yellow, orange, and red positive values). Among these regions are the Arctic Ocean, the Bay of Bengal, and the Northeast Atlantic and Mediterranean Seas.

The noisy appearance of the contours of certain (global) fields plotted with the GMT graphic tool is similar to the noise clearly existing in the

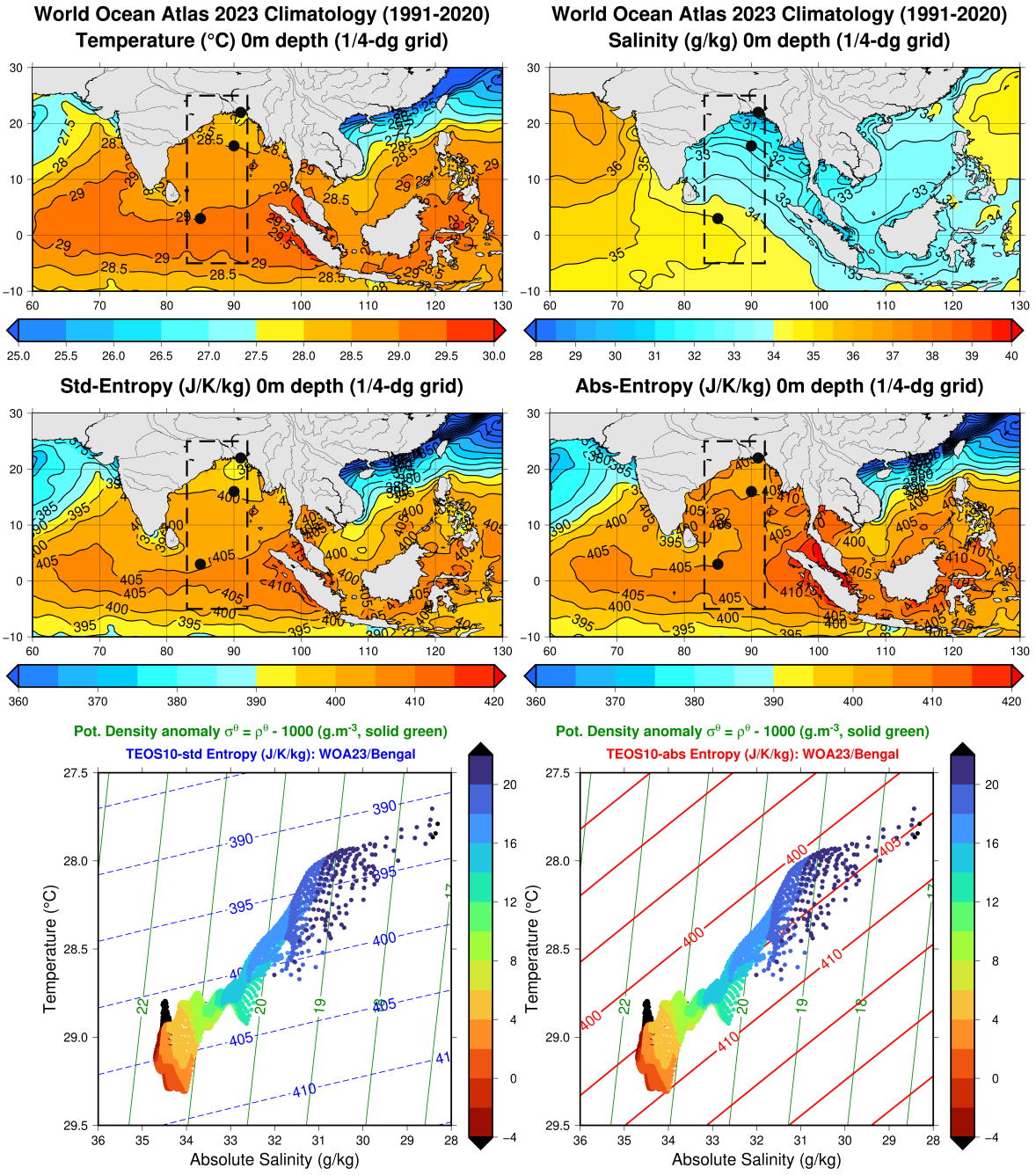

Figure 6. The same as in Figures 4, but for the Bay of Bengal and with three additional black disks at locations used to show numerical computations in the main text. Two $t - S_A$ diagrams are plotted with the TEOS standard-entropy blue-dashed lines (bottom left) and the absolute-entropy solid-red lines (bottom right). The disks are coloured according to the latitude scale values (from maroon for 4 dg south to dark blue for 24 dg north). Both salinity and temperature axes have been reversed, with decreasing values to the right and upward.

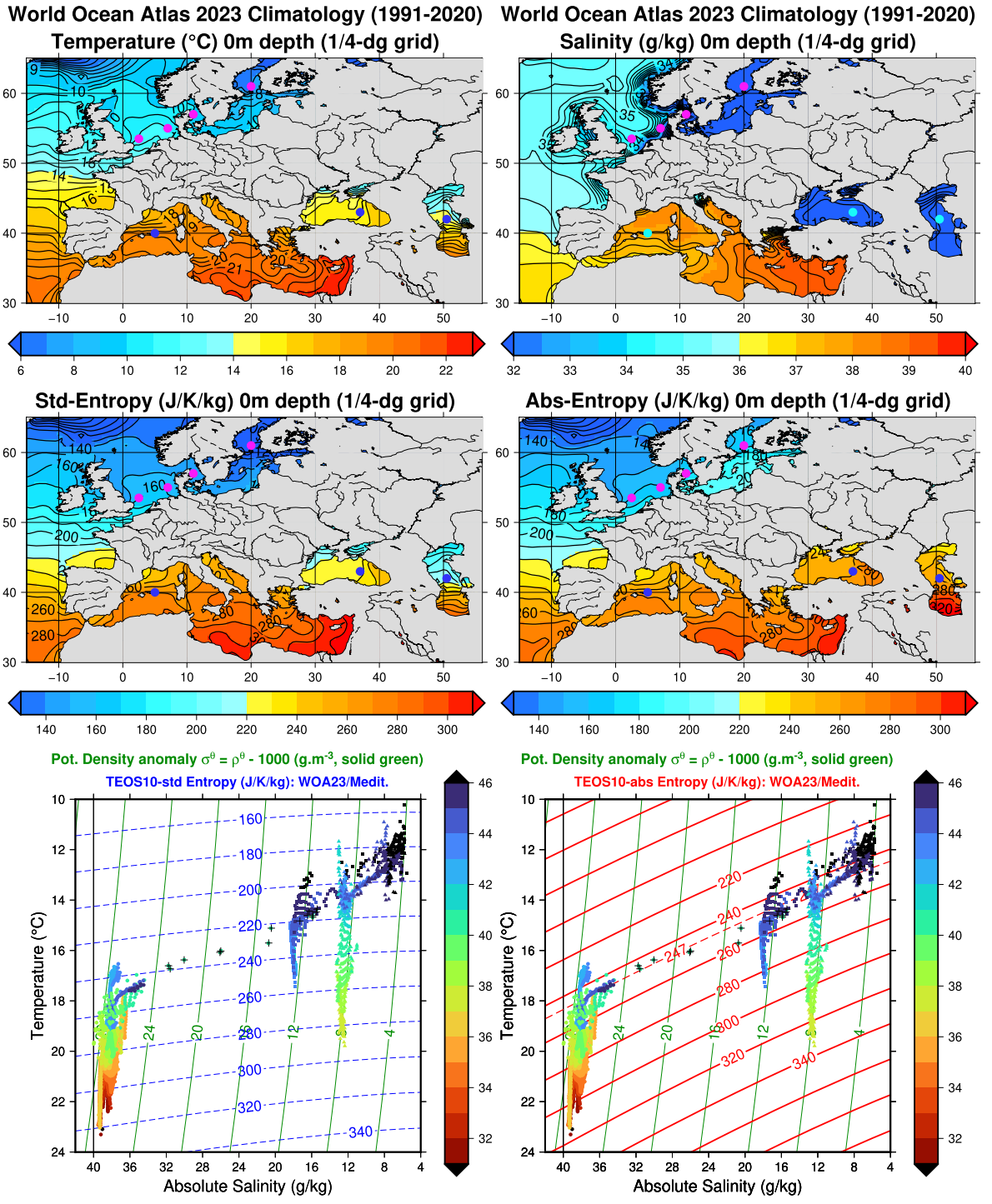

Figure 7. The same as in Figures 6, but for the Western Europe and North Africa domain and with seven magenta and blue disks. In the $t - S_A$ diagrams, the Mediterranean Sea (discs) is to the left, the Caspian Sea (triangle) to the right, and the Sea of Marmara (crosses) and Black Sea (squares) in between.

corresponding graphs (not shown) plotted directly from the WOA23 site and with the same quarter-degree resolution.

Note that the influence of non-linearities in the TEOS10 entropy formula is small (not shown), with similar values for the entropy $\eta(\overline{t}, \overline{S_A})$ computed from the annual mean values $\overline{t}$ and $\overline{S_A}$ for temperature and salinity, on the one hand, and for the mean entropy averaged from the 12 monthly mean values $\overline{\eta(t, S_A)}$, on the other hand.

2.4. *A study of surface entropy: Arctic Ocean*

The seawater standard (TEOS10) and absolute (third-law) entropies along the coasts of the Arctic Ocean are shown in the zoomed-in Figures 5.

The blue (<28 g·kg^{-1}) low values in salinity are due to the flow from the Mackenzie, Kolyma, Lena, Taz, and Ob rivers. The impacts of the associated large gradients in salinity correspond to more generalized (light-blue) absolute entropy values between 10 and 30 units off the coasts of Canada, Alaska, and Siberia, prolonging the same values off the west part of the Russian coasts (Barents and Kara Seas).

The surface values over the Arctic Ocean are thus more zonally symmetric with the absolute entropy than with the standard TEOS10 entropy. They are also more homogenized over the Bays of Hudson and Baffin, the Amundsen, Coronation, and Queen Maud Gulfs, and the Bering and Chukchi Seas. There are similarly more isentropic features in the Greenland Sea off the east coast of Greenland, where large gradients of salinity exist (see the dashed-black boxes).

The black line added to denote the Canada Basin (here at the longitude 140 E/220 W) roughly corresponds to the SCICEX'97 Transect-A (longitude 150 E/210 W), with the fresh water in the Beaufort Sea coming from the Mackenzie River. The larger (light-blue) annual-mean values for the absolute entropy are in agreement with the surface values in the right part of the SCICEX'97 Transects (A and B) shown in Figures 2 and 3.

2.5. *A study of surface entropy: Bay of Bengal*

The seawater standard (TEOS10) and absolute (third-law) entropies over the Bay of Bengal are shown in the zoomed-in Figures 6.

The low values of salinity (<32 g·kg^{-1}, in blue) are due to the flow from the Ganges and Brahmaputra rivers and deltas, located at the north of this bay of Bengal, and also at the east of this bay from the Irrawaddy, Sittang, and Salween rivers.

The impacts of the low values and large salinity gradients over the Bay of Bengal, associated with low values but smaller temperature gradients, are to homogenise the seawater absolute entropy within the broad 405-unit line (see the dashed boxes). The standard TEOS10 values exhibit larger north–south gradients with small values in the north of the Bay of Bengal and in the south with a narrow tongue formed by the 405 unit line corresponding to the 29 °C temperature line.

It is an interesting result to see how the waters to the north of the Bay of Bengal, with gradients in temperature and salinity, such as 27.7 °C and 27.8 g·kg^{-1}, 28.5 °C and 31.9 g·kg^{-1}, and 29.0 °C and 34.4 g·kg^{-1}, can produce such similar values of about 405 ± 0.2 J·K^{-1}·kg^{-1} only for the absolute thermodynamic formulation of seawater entropy (see the three black disks), and not for the present TEOS10's standard formulation of it, which varies by about 12 units (namely 391.3, 398.9, and 403.5 J·K^{-1}·kg^{-1}). This cannot be due to chance, and it will be needed to better understand in the future which physical processes may be responsible for such a peculiar homogenisation of seawater absolute entropy, despite and because of such a special combination of temperature and salinity gradients. It should be pointed out that the rule (6) for isentropic variations does not apply here, as this rule was only valid for temperatures close to zero Celsius, whereas here for $t \approx 28$ °C all the terms of the $\eta(x, y, z)$ formulation that are non-linear in $y = t/(40) \approx 0.7$ should be taken into account.

It is also interesting to study the two $t - S_A$ diagrams (see Part-I) shown at the bottom of Figures 6, with the same green (isopycnic) iso-potential-density lines but with either the standard, arbitrarily modified TEOS10 version of the seawater entropy (on the left, with blue shaded lines) or with the absolute thermodynamic entropy (on the right, with solid red lines). The seawater points plotted on these diagrams are those located within the domain (−5 dg/+25 dg) in latitude and (83 dg/92 dg) in longitude (see the dashed boxes in Figures 6).

The absolute seawater entropy, in accordance with thermodynamics, shows (on the right) a

remarkable but unexpected alignment of the points around the isentrope 405 ± 3 J·K^{-1}·kg^{-1} for almost all the latitudes, despite significant gradients in temperature and salinity. In a different way, the blue curves (on the left) drawn with the standard TEOS10 formulation, which for this high range of temperature and salinity have a slope about three times lower than for the absolute entropy, do not provide any particular physical information and have a clear decorrelation with the scatterplot.

This confirms, for these tropical conditions, the importance of plotting these red absolute isentropic lines on the $t - S_A$ diagrams, as already indicated when studying the polar SCICEX'96 and SCICEX'97 profiles. This also means that, since the increased slope of these absolute isentropes compared to the TEOS10 formulation is a direct consequence of the addition of the absolute entropy increment $\Delta\eta_s = (\eta_{s0} - \eta_{w0})(S_A - S_{SO})/1000$, which adds a linear function of the salinity depending on the reference values of the entropies η_{w0} of pure water and η_{s0} of sea salts, these values cannot be modified without physical consequences (as presently done with the TEOS10 formulation) on the calculation of the seawater entropy and second law.

2.6. *A study of surface entropy: Northeast Atlantic and Mediterranean Seas*

The seawater standard (TEOS10) and absolute (third-law) entropies over western and central Europe, northern Africa, and the western part of the Middle East are shown in the zoomed-in Figures 7.

In the Northeast Atlantic, colder temperatures with smaller salinity create more homogeneous absolute seawater entropy (light blue, between 170 and 190 units) over the Ireland Sea, off the whole coastal regions from south England and north of France (the English Channel), the south of the North Sea, Denmark (Skagerrak, Kattegat), the Baltic Sea, south of the Gulf of Bothnia, and up to the Gulf of Finland. These absolute-isentropic features do not exist for the standard TEOS10 seawater entropy, which has almost exactly the same uneven shape as the temperature field and which is continuously decreasing from west to east off these coastal regions. As an example (see the four magenta disks), the absolute entropy line 166 ± 0.1 J·K^{-1}·J·kg^{-1} corresponds to very different (t, S_A) conditions from west (North Sea) to east (Gulf of Bothnia): (11.5 °C, 34.5 g·kg^{-1}), (10.75 °C, 30 g·kg^{-1}), (10 °C, 25.5 g·kg^{-1}), and (7.2 °C, 5.9 g·kg^{-1}), with a clear decrease in standard (TEOS10) entropy by more than 53 units: 164.8, 156.5, 147.7, and 111.1 J·K^{-1}·J·kg^{-1}, respectively.

Note that there is no point over the Russian Rybinsk reservoir and lakes of Ladoga and Onega for the WOA23 quarter-degree resolution dataset (accordingly, I have masked these 3 regions).

Over the Mediterranean Sea, the NW/SE gradient of temperature and W/E gradient of salinity combine with each other to create a slightly smoother and more N/S gradient in seawater absolute entropy. The 260–270 units (orange) band extends at almost constant latitude in the whole Mediterranean Sea (from Barcelona, Naples, Athens, and Istanbul). There is, moreover, an unexpected extent toward the Black and Caspian Seas, which have especially low values of salinity and similar absolute seawater entropy as in the Mediterranean Sea. These features do not exist for the standard (TEOS10) seawater entropy, which again has almost exactly the same uneven shape as the temperature field, and thus with less homogeneous values for the Mediterranean, Black, and Caspian Seas.

Note that there is no point over the Aral Sea for the WOA23 quarter-degree resolution dataset (not shown). Note also that the relevance of the TEOS10 formulation to compute the entropy of low-salinity lakes (like here for the Caspian Sea) has been recalled by Feistel (2018, p. 477), who stated that: "*based on the heuristic, empirical "Millero rule", which argues "that the physical chemical properties of most lakes can be determined from equations for seawater at the same total salinity" (…) the properties of anomalous seawater can be estimated by the TEOS-10 functions in terms of SSW properties evaluated at the same density, temperature, and pressure.*"

To confirm and better illustrate these unexpected and astonishing almost absolute-isentropic states for these three Mediterranean, Black, and Caspian Seas, the three typical conditions (19.0 °C, 38.3 g·kg^{-1}), (15.4 °C, 18.0 g·kg^{-1}), and (14.5 °C, 12.2 g·kg^{-1}), corresponding to the three (east/west) blue disks in Figures 7, lead to similar values of absolute entropy (260 ± 0.2 J·K^{-1}·kg^{-1}). Differently, the standard (TEOS10) entropies are decreasing by about 50 units (266.3, 227.5, and 216.7 J·K^{-1}·kg^{-1}).

As with the Bay of Bengal (Figures 6), it is also useful to study the $t - S_A$ diagrams shown at the bottom of Figures 7 with points coloured by latitudes (from maroon for 31 dg north to dark blue for 46 dg north) for the Mediterranean Sea (discs), the Black Sea (squares), the Caspian Sea (triangles), and the Sea of Marmara (crosses). The smaller latitude points are roughly aligned along isopycnic green lines: the Mediterranean Sea has the higher density (26–30 g·kg^{-1}), the Caspian Sea the smaller density (8–9 g·kg^{-1}), with the Black Sea in between (12–13 g·kg^{-1}) and the Sea of Marmara connecting the Mediterranean and Black Seas (rapid variations between 24 and 12 g·kg^{-1}).

Clearly the standard values of the TEOS10 entropy (blue dashed lines, on the left) are not correlated with the Mediterranean, Marmara, Caspian, and Black Sea scatterplots. Differently, the new absolute seawater entropy red lines (on the right) roughly connect the points at the same latitude and colours. Moreover, there are unexpected absolute isentropic rough alignments of the higher (northern, blue, and dark-blue) symbols along the 247 absolute entropy dashed-red line, including the connecting Marmara's crosses. Since the red absolute entropy lines are unknown to the WOA23 objective analysis process, this means that nature has chosen to follow either the isopycnic green lines (for the lowest latitudes) or the red absolute seawater entropy lines (for the highest latitudes), with no bias due to the WOA23 processes acting separately on t and S_A.

As with the Bengal Sea and the absolute entropy of the atmosphere, this means, on the one hand, that the absolute entropy defined in thermodynamics has a hidden physical meaning, which is revealed here by the $t - S_A$ oceanic diagrams. On the other hand, it is not possible to arbitrarily modify the increment $\Delta\eta_s$ by freeing oneself from the use of the reference values of entropies, as recommended by the third law and provided in all the Tables of Thermodynamics.

Note that the more zonally symmetric feature of the 240–260 entropy-unit band cannot be explained by pure oceanic processes, simply because the Caspian Sea does not communicate with the two other seas, the Black and Mediterranean Seas. Therefore, it will be needed to better understand in the future which physical processes may be responsible for such a peculiar homogenisation of absolute seawater entropy. For instance, this may be due to more general and zonally symmetric atmospheric processes and via the interface between the atmosphere and the ocean.

3. Conclusion

In this Part II, the absolute seawater entropy η_{abs} defined in Part I is studied for the first time with concrete case studies and applications to oceanic vertical CTD profiles and analysed surface datasets. The absolute entropy η_{abs} recalled in (1) is computed by adding the salinity increment $\Delta\eta_s$ recalled in (5) to the standard TEOS10 value $\eta_{std/TEOS10}$ recalled in Part I.

The case studies undertaken in this Part II reveal new homogeneous and isentropic features, both vertically and horizontally at the surface, with the property that only the absolute version of the seawater entropy can reveal these new isentropic regions.

These peculiar absolute-isentropic features are clearly visible on the three oceanic $t - S_A$ diagrams studied for polar (SCICEX'96 and 97), tropical (Bay of Bengal), and mid-latitude (Mediterranean, Marmara, Black, and Caspian Seas) conditions. The scatterplots appear to preferentially follow either iso-potential-density green lines or iso-absolute-entropy red lines, to the exclusion of the blue lines and the "arbitrarily modified seawater entropy" presently offered as an output of TEOS10. These results could not have been obtained by randomly juxtaposing oceanic states with very different temperatures and salinities and leading (by chance) to the same absolute-entropy values.

Generally speaking, it was worth studying the impact of the increment term $\Delta\eta_s$ wherever salinity values are particularly low or high, but also wherever salinity gradients are large. It can even be said, insofar as the TEOS10 formulation leads to almost the same spatial structures as for temperature, that there is very little advantage in proposing the current standard entropy field as an output of TEOS10.

Differently, the absolute entropy field, including the thermodynamically consistent increment term $\Delta\eta_s$, seems to provide a real added value, which should justify its calculation and its availability as an output of TEOS10. But there is nothing surprising in this, since absolute entropy is one of the fundamental quantities of thermodynamics (along with temperature and energy), and only the inclusion of this

increment $\Delta\eta_s$ makes it possible to calculate this entropy rigorously for the seawater, as prescribed by the third law of thermodynamics, which cannot be called into question with impunity (as done in TEOS10).

Possible physical explanations for these alignments along absolute isentropes may include turbulent processes occurring in the atmosphere, in the oceans, and at the interfaces between the two. Indeed, partly suggested by my earlier studies of the absolute entropy of the atmosphere, this uniformity of absolute seawater entropy, and therefore the isentropic status of surface waters, may be due to atmospheric turbulent processes following the recommendations of Richardson (1919) and Richardson (1922). He explained that the atmospheric turbulence must involve the wind components, the total water content, and the absolute entropy (or the associated potential temperature). In line with this hypothesis, I have shown that turbulent schemes are preferentially applicable to the absolute entropy for the atmosphere (Marquet, 2011; Marquet and Bechtold, 2020) and for oceanic bulk schemes (Marquet and Belamari, 2017), with in all probability the same turbulent processes that should be applied to the absolute seawater entropy (and not to the temperature t nor the actual potential temperatures θ or Θ).

Therefore, a possible interpretation for these isentropic oceanic structures may be found in the more homogeneous and zonally symmetric atmospheric circulation and in the corresponding impacts on the oceanic state variables via the bulk-surface turbulent processes acting on the absolute entropy. Note, however, that the turbulence processes applied to absolute entropy do not prevent but add to the impacts linked to convective phenomena, which are linked to buoyancy and density-related variables (such as virtual temperature for the atmosphere and isopycnic lines for the ocean). It could therefore be imagined a sort of competition between these two turbulent and convective effects, acting on different variables, as shown by the scatterplots on the $t - S_A$ diagrams, which follow one or the other of the families of green (isopycnic) or red (absolute-isentropic) curves.

It should be emphasized that the correction term $\Delta\eta_s$ depends linearly on salinity and thus varies not only spatially but temporally, which fundamentally changes the calculation of entropy itself beyond the addition of a simple constant (like η_{w0} in η^{W}_{Fei03} recalled in Table 1 of Part I). Consequently, studies of the type "maximum entropy state" defined by $d\eta = 0$ depend on a certain combination of the differentials dT and $(\eta_{w0} - \eta_{s0})\, dS_A$. There is, therefore, an impact of the absolute reference entropy terms η_{w0} and η_{s0} for non-stationary states with both $dT \neq 0$ and $dS_A \neq 0$, as, for example, for the regional, seasonal, and climate changes.

Furthermore, insofar as the entropy gradient regions influence the turbulent transport of this thermodynamic state variable, with turbulent flows that must cancel out in isentropic regions, the absolute definition of entropy must be preferred to any other arbitrarily modified definition; otherwise, the entropy budget and therefore the second principle of thermodynamics will be arbitrarily modified. In fact, the entropy balance equation cannot be reduced to the positive production term usually studied, and entropy flows (often discarded) at the ocean-atmosphere interface depend on $\Delta\eta_s$ and on the absolute definition of entropy studied in the paper.

This study should be continued in order to better understand the origin of the zonally symmetric and local three-dimensional oceanic structures of the absolute seawater entropy, in particular in the Bay of Bengal, in the Mediterranean, Black, and Caspian Seas, the Northeast Atlantic and Mediterranean Seas, as well as in the whole Arctic Ocean.

Acknowledgments

The author would like to thank the anonymous referees and the editor for the constructive comments, which help to improve the manuscript.

I would also like to extend my warmest thanks to Jean-Claude André, whose invaluable and crucial assistance made it possible to publish both parts of this paper.

The Fig. 1 by Steele et al. (2004, p. 2) is free of Copyright by the AGU (*J. Geophys. Res. Oceans*). The SCICEX'96 and 97 CTD vertical profiles and SCICEX'97 Sample Locations map have been downloaded in September 2024 at: https://nsidc.org/scicex and https://www.nodc.noaa.gov/archive/arc0021/0000568/1.1/data/0-data/, see the Supplementary Data.

The World Ocean Atlas 2023 climatology (WOA23, release February 2024, quarter-degree grid) are freely available at: https://www.ncei.noaa.gov/products/world-ocean-atlas.

The TEOS10-GSW Oceanographic FORTRAN software has been downloaded from https://www.teos-10.org/software.htm (McDougall and Barker, 2011).

Declaration of interests

The author does not work for, advise, own shares in, or receive funds from any organization that could benefit from this article, and has declared no affiliations other than their research organization.

Supplementary data

The SCICEX and WOA23 directories were broken in October 2024 due to Hurricane Helene Outage. I have made available in the Zenodo site (Marquet, 2024a; Marquet, 2024b) the SCICEX (96 and 97) CTD and WOA23 public sub-datasets used to plot the Figures 1–7.

Supplementary materials are provided in the Zenodo file (Marquet, 2025).

References

Feistel, R., "Thermodynamic properties of seawater, ice and humid air: TEOS-10, before and beyond", *Ocean Sci.* **14** (2018), no. 3, pp. 471–502.

Marquet, P., "Definition of a moist entropy potential temperature: application to FIRE-I data flights", *Quart. J. R. Meteorol. Soc.* **137** (2011), no. 656, pp. 768–791.

Marquet, P., *Supplementary Materials about absolute (third-law) atmospheric and seawater entropies and enthalpies*, Zenodo, 2025. Online at https://doi.org/10.5281/zenodo.17639497 (accessed on April 7, 2026).

Marquet, P., "The absolute seawater entropy: Part I. Definition", *C. R. Géosci.* (2026). Online at https://doi.org/10.5802/crgeos.333.

Marquet, P., *SCICEX CTD files 96 (cast-43) and 97 (CTD_xxx.EDF) [Data set]*, Zenodo, 2024a. Online at https://doi.org/10.5281/zenodo.13869779 (accessed on April 7, 2026).

Marquet, P., *World Ocean Atlas 2023 (WOA23) 1991–2020 (t, Sa, d) annual means [Data set]*, Zenodo, 2024b. Online at https://doi.org/10.5281/zenodo.13895641 (accessed on April 7, 2026).

Marquet, P. and P. Bechtold, "A new Estimated Inversion Strength (EIS) based on the moist-air entropy", in *Research Activities in Atmospheric and Oceanic Modelling. WRCP-WGNE Blue-Book Report No 12/2020* (Astakhova, E., ed.), vol. 10, WMO: Geneva, 2020, pp. 1–2. Online at http://bluebook.meteoinfo.ru/uploads/2020/docs/04_Marquet_Pascal_NewEntropyEIS.pdf (accessed on April 7, 2026).

Marquet, P. and S. Belamari, "On new bulk formulas based on moist-air entropy", in *Research Activities in Atmospheric and Oceanic Modelling. WRCP-WGNE Blue-Book* (Astakhova, E., ed.), vol. 4, WMO/ICSU/IOC, 2017, pp. 9–10. Online at http://bluebook.meteoinfo.ru/uploads/2017/docs/04_MARQUET_Pascal_moist_entropy_bulk.pdf (accessed on April 7, 2026).

McDougall, T. J., "Potential enthalpy: a conservative oceanic variable for evaluating heat content and heat fluxes", *J. Phys. Oceanogr.* **33** (2003), no. 5, pp. 945–963.

McDougall, T. J. and P. M. Barker, *Getting started with TEOS-10 and the Gibbs Seawater (GSW) Oceanographic Toolbox*, SCOR/IAPSO WG127, 2011. Online at https://www.teos-10.org/pubs/Getting_Started.pdf (accessed on April 7, 2026). ISBN 978-0-646-55621-5 p. 28.

McDougall, T. J., P. M. Barker, R. Feistel and F. Roquet, "A thermodynamic potential of seawater in terms of absolute salinity, conservative temperature, and in situ pressure", *Ocean Sci.* **19** (2023), no. 6, pp. 1719–2013.

McDougall, T. J., R. Feistel, D. G. Wright, et al., "The International Thermodynamic Equation of Seawater - 2010: Calculation and Use of Thermodynamic Properties", in *TEOS-10 Manuals and Guides No. 56*, UNESCO, SCOR and IAPSO: Paris, France, 2010, 208 pp. Online at http://www.teos-10.org/pubs/TEOS-10_Manual.pdf (accessed on April 7, 2026). Intergovernmental Oceanographic Commission.

Richardson, L. F., "Atmospheric stirring measured by precipitation", *Proc. R. Soc. Lond. A* **96** (1919), no. 674, pp. 9–18.

Richardson, L. F., *Weather Prediction by Numerical Process*, Cambridge University Press: Cambridge, 1922, p. 236. Online at https://archive.org/details/weatherpredictio00richrich (accessed on April 7, 2026).

Steele, M., J. Morison, W. Ermold, I. Rigor, M. Ortmeyer and K. Shimada, "Circulation of summer Pacific halocline water in the Arctic Ocean", *J. Geophys. Res.: Oceans* **109** (2004), no. C02027, pp. 1–18.